Acta Crystallographica Section D
Biological Crystallography
ISSN 0907-4449

An unusual case of pseudo-merohedral twinning in orthorhombic crystals of Dicer

Ian J. MacRae[a,b] and Jennifer A. Doudna[a,b]*

[a]Howard Hughes Medical Institute, Departments of Molecular and Cell Biology and Chemistry, University of California, Berkeley, CA 94720, USA, and [b]Physical Biosciences Division, Lawrence Berkeley National Laboratory, Berkeley, CA 94720, USA

Correspondence e-mail: doudna@berkeley.edu

Received 16 May 2007
Accepted 23 July 2007

PDB Reference: Dicer, 2qvw, r2qvwsf.

The crystal structure of the enzyme Dicer from *Giardia intestinalis* was solved to 3.3 Å resolution by MAD using crystals belonging to space group $P2_12_12$ [Macrae *et al.* (2006), *Science*, **311**, 195–198]. These crystals were derived from crystals that diffracted X-rays to 3.0 Å resolution but were refractory to structure determination because they were twinned. It is shown here that the original Dicer crystals represent an unusual case of perfect pseudo-merohedral twinning of orthorhombic crystals. Before the twinning problem was overcome, it was possible to calculate a low-resolution electron-density map in space group $P4_1$ that was used to build a partial molecular model. Experimental phases were sufficient to identify heavy-atom sites that indicated space-group inconsistency, leading to identification of the true space group. This information guided the search for different crystallization conditions that yielded untwinned crystals and ultimately a fully interpretable electron-density map.

1. Introduction

RNA interference (RNAi) is a widespread eukaryotic regulatory process in which double-stranded RNA (dsRNA) triggers the silencing of cognate genes. The initiation of RNAi and related gene-silencing pathways requires the cleavage of cellular or viral dsRNA into small RNA fragments ~21–27 nucleotides in length by the enzyme Dicer (Bernstein *et al.*, 2001; Ketting *et al.*, 2001). We previously determined the crystal structure of a Dicer enzyme from *Giardia intestinalis* at 3.3 Å resolution and proposed a structural model for dsRNA processing (Macrae *et al.*, 2006).

The *Giardia* Dicer crystals used for structure determination were only obtained after extensive optimization of crystals that were discovered to be pseudo-merohedrally twinned. Merohedral twinning, which is relatively common in both small-molecule and protein crystallography, occurs when crystals contain lattices of separate twin domains that superimpose perfectly in three dimensions. In this situation, the unit-cell orientation produced by the twinning operation still fits into the original unit-cell lattice, yet the orientation of the molecules in the two unit cells is not equivalent. This scenario generally holds true only for a limited set of high-symmetry space groups (tetragonal, trigonal, hexagonal and cubic) in which the space-group symmetry is lower than the lattice symmetry (Yeates, 1997). In rare cases, merohedral twinning also occurs in lower symmetry space groups where the unit-cell geometry closely resembles one with high symmetry, such as orthorhombic or monoclinic space groups in which two of the unit-cell axes are equivalent. In some cases, structures have been solved using such twinned data even when the twin

fraction α was close to 0.5 (see, for example, Rudolph *et al.*, 2004; Wittmann & Rudolph, 2007).

Here, we present the clues that led to the identification of pseudo-merohedral twinning during the MAD structure determination of Dicer. Electron-density maps calculated using the wrong space group produced partially interpretable density for one of the molecules in the crystallographic asymmetric unit, enabling the detection of space-group inconsistency with the heavy-atom positions. The Dicer structure was ultimately solved using untwinned crystals produced by modification of the original crystallization conditions. This study suggests approaches that may be useful for other MAD structure determinations involving twinned crystals.

2. Experimental

2.1. Data collection

The expression, purification and crystallization of full-length *G. intestinalis* Dicer (85 kDa, 754 residues), as well as the MAD structure determination using an $ErCl_3$ derivative, have been described previously (Macrae *et al.*, 2006). Crystals grown in the presence of $MgCl_2$ were almost perfectly pseudo-merohedrally twinned, whereas those grown in the presence of $MnCl_2$ were macroscopically twinned and could be dissected into single-crystal shards (Macrae *et al.*, 2006). Diffraction data were measured at beamlines 8.2.1 and 8.2.2 at the Advanced Light Source, Lawrence Berkeley National Laboratory.

2.2. Data analysis and phasing

Data were processed using *DENZO*/*SCALEPACK* (Otwinowski & Minor, 1997). The positions of the Er atoms were located using the program *HySS* (Adams *et al.*, 2004) and were refined with *SHARP* (Vonrhein *et al.*, 2006) or *MLPHARE* (Potterton *et al.*, 2002, 2004) using *ELVES* (Holton & Alber, 2004). Density modification was performed using *DM* (Potterton *et al.*, 2002, 2004).

2.3. Refinement against twinned data

The model of Dicer (PDB code 2ffl; originally built and refined to 3.3 Å resolution using untwinned crystals) was refined against the original structure factors of the native twinned data in *CNS* (Brünger *et al.*, 1998) using model structure factors to estimate the untwinned structure factors, which were then used as the target for refinement. The model was subsequently refined against pseudo-merohedrally twinned data to a resolution of 3.0 Å using *CNS*. The twinning operator (l, $-k$, h) and a twin fraction of 0.5 were used in refinement.

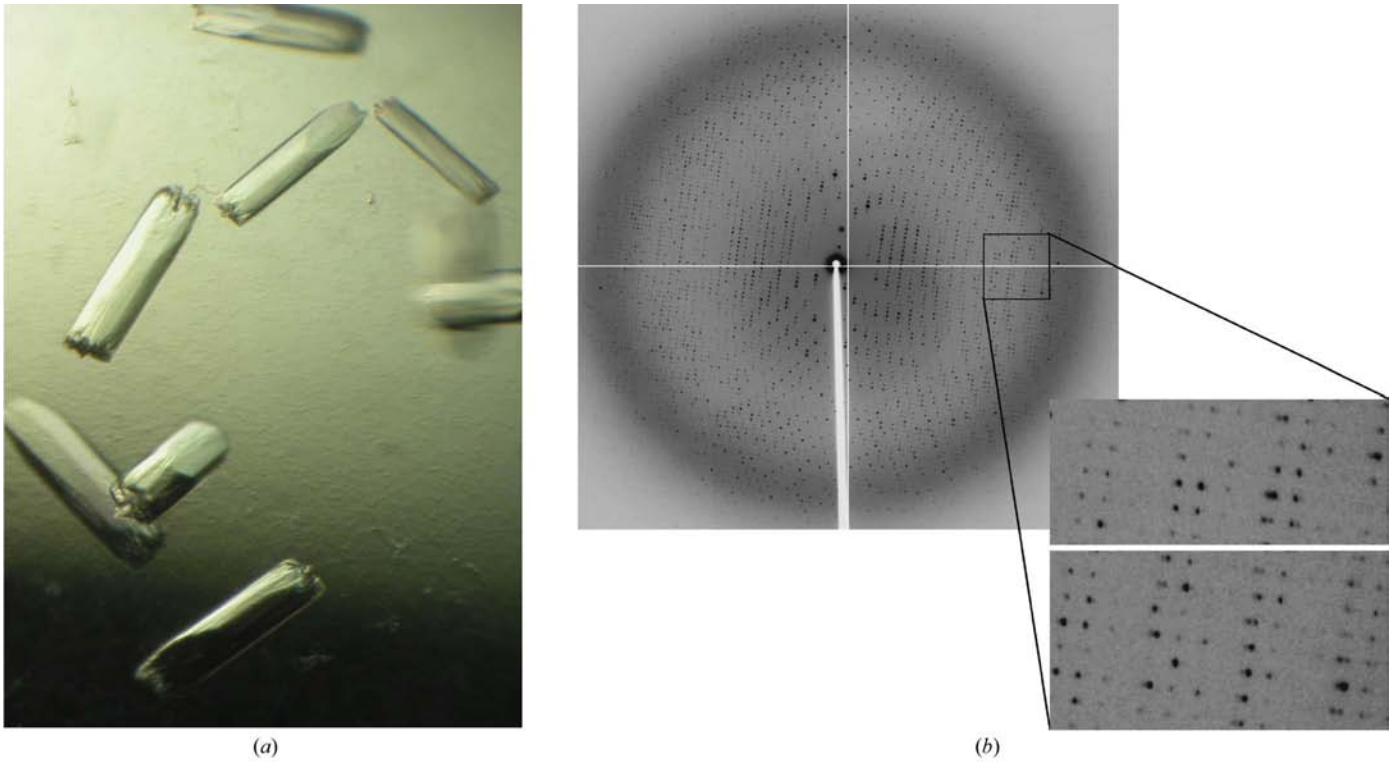

Figure 1
Original twinned crystals obtained of *Giardia* Dicer. (*a*) Crystals grew to typical dimensions of 50 × 50 × 200 µm. (*b*) A diffraction pattern obtained at beamline 8.2.1 at the Advanced Light Source, Lawrence Berkeley National Laboratory. The spot profiles from two twinning domains overlap nearly perfectly, although some split spots are observed (enlarged inset).

Table 1
Statistics from twinned data processed in three space groups.

Values in parentheses are for the highest resolution shell.

Space group	$P222_x$	$P4_x$	$P4_x22$
Resolution (Å)	3.0 (3.1–3.0)	3.0 (3.1–3.0)	3.0 (3.1–3.0)
Redundancy	8.2 (8.3)	8.5 (8.5)	16.2 (16.4)
Completeness (%)	100 (100)	100 (100)	100 (100)
$R_{\rm merge}$†	8.9 (43.8)	9.1 (43.1)	9.3 (44.1)
$I/\sigma(I)$	25.3 (5.6)	25.5 (5.9)	34.9 (8.3)
Unit-cell parameters			
a (Å)	155.5	155.5	155.5
b (Å)	155.5	155.5	155.5
c (Å)	173.5	173.5	173.5
Wilson B (Å^2)	68.7	68.6	68.4
$\langle I^2\rangle/\langle I\rangle^2$	1.66	1.69	1.64

† $R_{\rm merge} = (\sum_h \sum_i I_h - I_{hi}/\sum_h \sum_i I_{hi}) \times 100$, where I_h is the mean of I_{hi} observations of reflection h.

3. Results and discussion

3.1. Initial data analysis

G. intestinalis Dicer crystallized as ragged rod-shaped oblong crystals with typical dimensions of 200 × 50 × 50 µm (Fig. 1*a*). Crystallization was absolutely dependent on the presence of 2–10 m*M* of the reducing agent tris(2-carboxyethyl)phosphine hydrochloride (TCEP) in the mother liquor. Dithiothreitol (DTT) could not substitute for TCEP. Some of the high-resolution diffraction peaks were split, but this was not the case for every crystal or for all peaks (Fig. 1*b*). The data sets used for analysis did not contain split diffraction spots. Pseudo-merohedral twinning was recognized after numerous native and derivative data sets had already been collected. Up to this point, the space group had been tentatively assigned as either $P4_122$ (or $P4_322$) or $P4_1$ (or $P4_3$). Twinning could not be detected from molecular-packing considerations, as the large asymmetric unit allowed the presence of four NCS-related molecules for space group $P4_1$ or two molecules for space group $P4_122$, each resulting in a reasonable Matthews coefficient (3.1 Å^3 Da^{-1} with a solvent content of 60.6%).

Structure determination was begun using data measured from native and Er^{3+}-derivatized twinned crystals. Data processing resulted in similar $R_{\rm sym}$ values for the space groups $P222_1$, $P4_1$ and $P4_122$ using the native data, suggesting that the highest symmetry space group was correct (Table 1). The observed diffraction intensities were analyzed using *DETWIN* (Taylor & Leslie, 1998), an algorithm that checks for twinning by evaluating whether the cumulative intensity distribution follows Wilson statistics (Wilson, 1949; Dauter, 2003). Because twinned crystals give rise to diffraction intensities that show a characteristic deviation in the numbers of strong, medium and

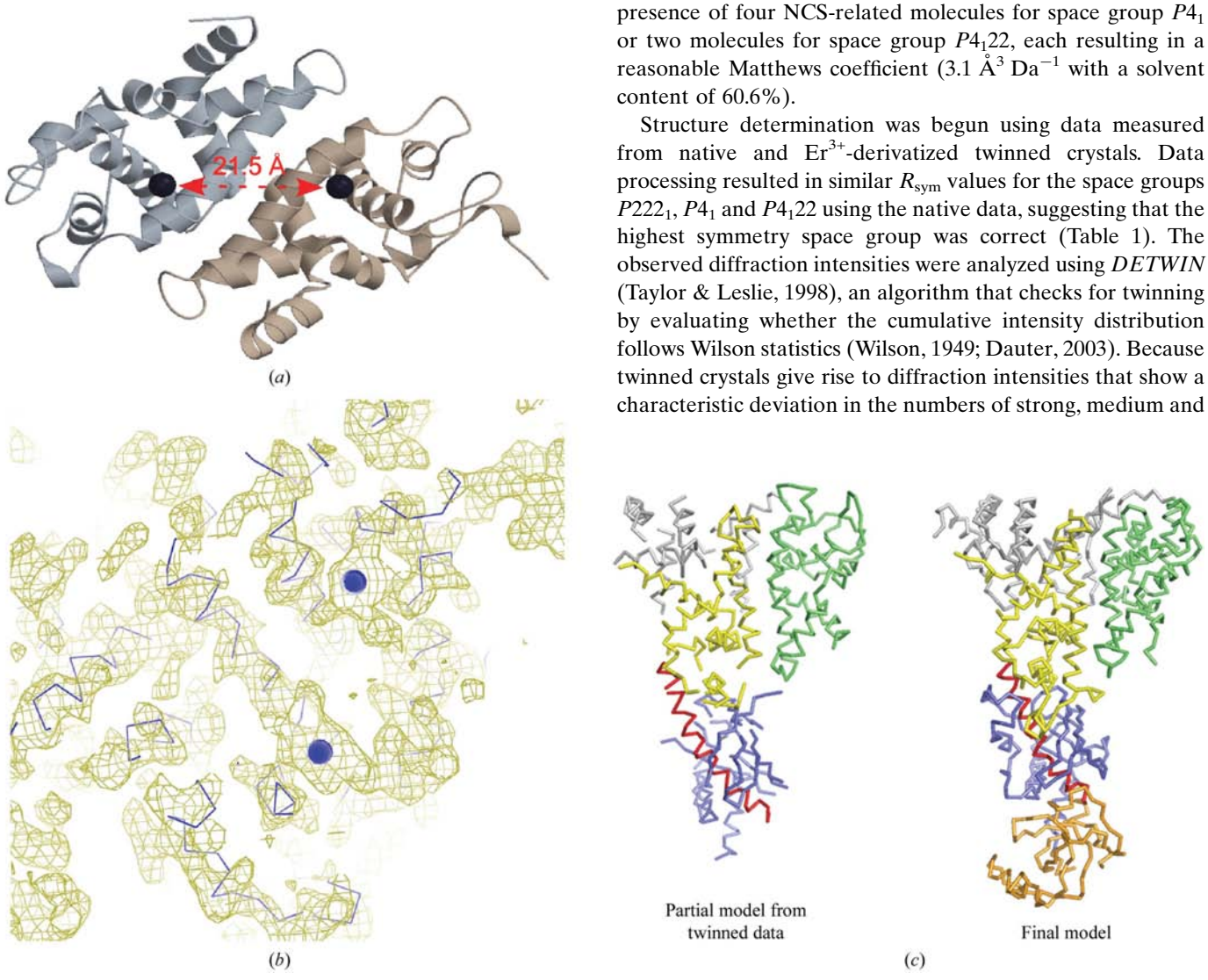

Figure 2
Heavy-atom sites identified in space group $P4_1$. (*a*) Distance between divalent metal ion-binding sites in the dimeric structure of bacterial ribonuclease III (Blaszczyk *et al.*, 2001). (*b*) Docking of the ribonuclease III structure (Blaszczyk *et al.*, 2001) into an electron-density map calculated at 3.8 Å resolution using diffraction data from twinned Er^{3+}-derivatized crystals processed in space group $P4_1$. (*c*) Polyalanine model of Dicer built into a 3.8 Å $P4_1$ electron-density map (left) compared with the final model from untwinned crystals (right).

weak intensities, twinning can be identified by calculating the second moment of intensities $\langle I^2\rangle/\langle I\rangle^2$ for narrow resolution bins (Yeates, 1988, 1997; Yeates & Fam, 1999; Padilla & Yeates, 2003). For acentric data, the expected value is 2.0 in the absence of merohedral twinning and 1.5 for perfect merohedral twinning. Intermediate values can potentially arise for twinned crystals that also have noncrystallographic pseudo-translational symmetry, which can systematically alter the number of very weak reflections and thereby increase the value that would otherwise be calculated for twinned data (Barends & Dijkstra, 2003). The intermediate $\langle I^2\rangle/\langle I\rangle^2$ value of 1.7 calculated for the Dicer data therefore indicated a possible twinning problem.

3.2. Identification of pseudo-merohedral twinning during MAD analysis

The heavy-atom sites used for phasing were identified by *HySS* and refined in *SHARP* using two-wavelength MAD data measured from an $ErCl_3$-soaked twinned crystal. Eight strong Er^{3+} sites were found (>8σ) and when displayed in the $P4_1$ unit cell revealed a distinctive geometry in which pairs of sites were located ∼21 Å apart. These distances were equivalent to those observed between divalent metal ions bound in the catalytic centers of bacterial ribonuclease III (Blaszczyk *et al.*, 2001), an enzyme whose catalytic domains are highly homologous to the catalytic domains of Dicer (Fig. 2*a*). Electron-density maps calculated at 3.7 Å resolution using the phases from these sites showed reasonable density surrounding four of the Er^{3+} ions. The site geometry, together with the fact that each Dicer protein sequence contains two RNase III domains, suggested that four Dicer molecules, each containing an RNase III 'dimer', might be included in the crystallographic unit cell. Based on this idea, it was possible to dock a backbone model of RNase III into the electron density with good agreement near the Er^{3+} sites (Fig. 2*b*). For one of the pairs of Dicer molecules, a polyalanine model that was almost 80% complete was built into the surrounding density, including areas outside

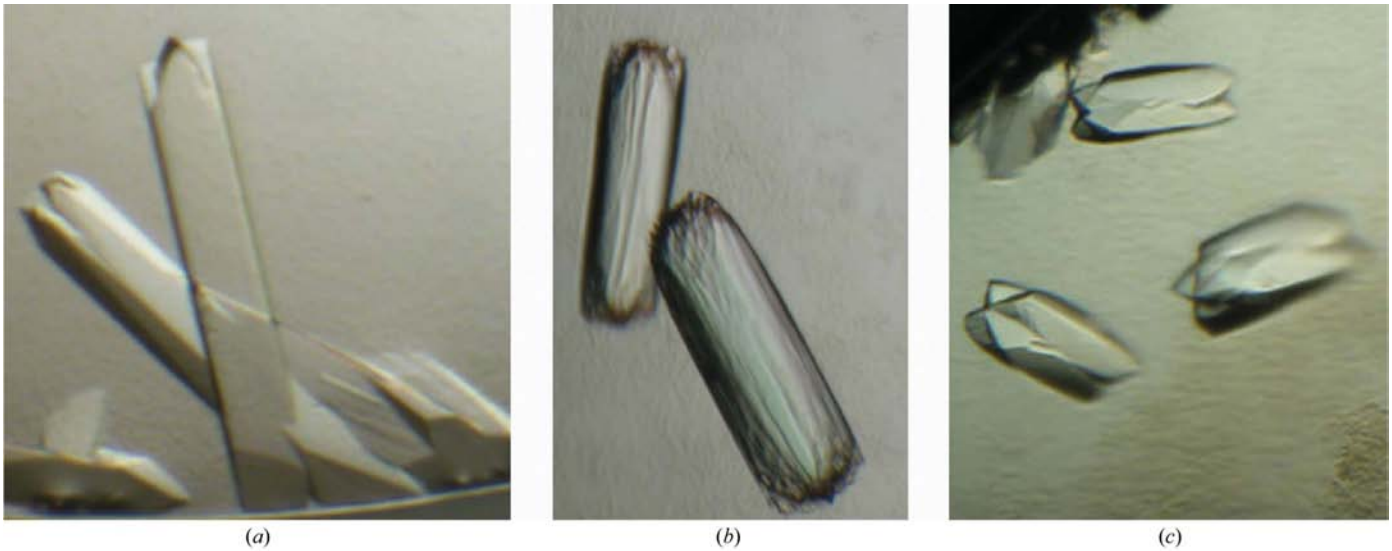

Space group	R_{sym}
*P*222	6.5
*P*422	38.0

(*d*)

Space group	R_{sym}
*P*222	4.7
*P*422	36.7

(*e*)

Space group	R_{sym}
*P*222	4.6
*P*422	4.8

(*f*)

Figure 3
Morphology and analysis of Dicer crystals grown in the presence of various divalent cations. Dicer crystals were obtained in the presence of (*a*) $BaCl_2$, (*b*) $MgCl_2$ (original conditions), (*c*) $MnCl_2$. (*d*–*f*) Diffraction data were measured from a dissected crystal shown in (*c*) by focusing incident X-rays on the regions indicated by the white circles. Symmetry *R* factors are shown for data processed in tetragonal *versus* orthorhombic space groups.

of the RNase III-homologous region. Although the majority of the amino-acid side chains could not be assigned, this crude model revealed the overall shape and some features of the Dicer protein (Fig. 2*c*).

However, density in some areas of the map was completely uninterpretable. This included the region surrounding four of the Er^{3+}-ion sites. More disturbingly, a third set of four Er^{3+} sites was detected in difference Fourier syntheses using phases from the original eight heavy-atom sites. The geometry of these additional sites was similar to that of the original sets, but superposition of the backbone model by alignment of the heavy-atom sites produced a major steric clash of symmetry-related molecules in the $P4_1$ unit cell.

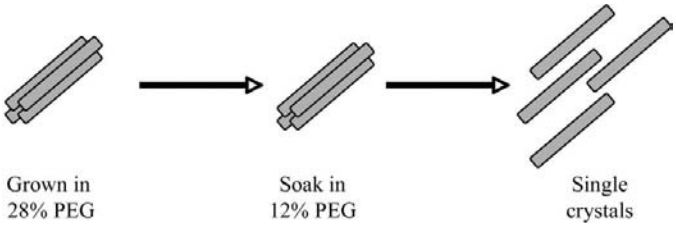

Figure 4
Method for dissecting macroscopically twinned Dicer crystals. Crystals grown in 28% polyethylene glycol (PEG) in the presence of $MnCl_2$ were transferred briefly to a solution containing 12% PEG, followed by dissection using a nylon loop. The separated single crystals could then be mounted individually for diffraction data collection.

Suspecting that the apparent fourfold axis of symmetry might be the result of twinning, a wide variety of new crystallization conditions were explored. We found that $MgCl_2$, which was required for growth of the original crystals, could be replaced by $BaCl_2$ or $MnCl_2$ to produce crystals with altered morphology (Figs. 3*a*, 3*b* and 3*c*). Crystals grew larger and with smooth faces in the presence of $BaCl_2$, but diffraction data analysis revealed that these crystals were isomorphous to the original crystals and therefore possibly subject to the same potential twinning problem. However, crystals grown in the presence of $MnCl_2$ had a distinctive four-lobed appearance that resembled epitaxic twinning (Fig. 3*c*). We hypothesized that these crystals might have reduced twinning relative to the original crystals and, if so, that each of the four lobes of an Mn-grown crystal might correspond to a single untwinned crystal. To test this possibility, an Mn-containing crystal was partially dissected using a cat whisker and mounted in a nylon loop with the junction between two lobes centered in the loop (Figs. 3*d*, 3*e* and 3*f*). Manual dissection of the crystals was difficult and the crystals were heavily damaged during the process. However, the partially dissected crystals still diffracted X-rays to 6 Å resolution, which was sufficient for crystal-system assignment. 180° of diffraction data were measured by focusing the X-ray beam on one lobe or the other or at the lobe junction and symmetry *R* factors were compared after data reduction in tetragonal *versus* orthorhombic space groups (without taking into account the potential effects of different degrees of redundancy, an issue that has been discussed recently; Weiss, 2001).

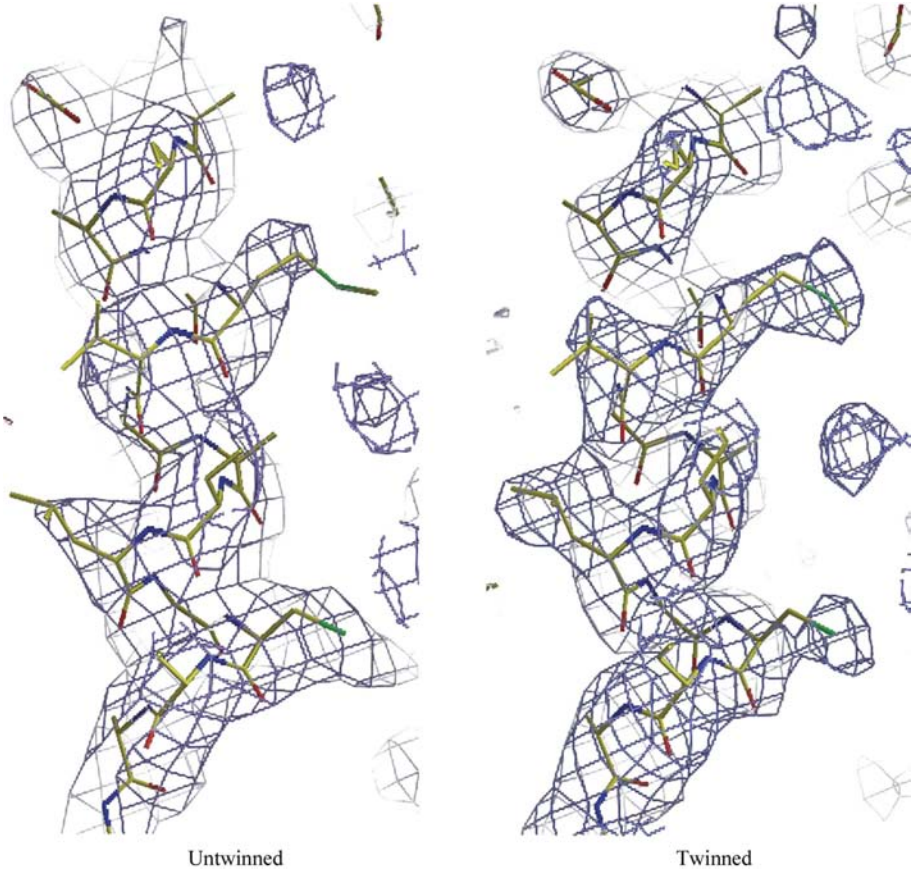

Figure 5
Electron-density maps ($2F_o - F_c$) contoured at 1σ calculated from untwinned (left) and twinned data sets (right). Maps from twinned data contained more features, but were less reliable than those from untwinned data.

This analysis demonstrated that data measured from either individual lobe had orthorhombic symmetry (Figs. 3*d* and 3*e*), whereas data measured from the lobe junction, which contained overlapping contributions from both lobes, showed tetragonal symmetry analogous to the data measured from the original crystals (Fig. 3*f*). This diffraction analysis was critical to identifying the macroscopic twin domains because the Dicer crystals are not highly birefringent, and it was not possible to distinguish separate twin domains under polarized light. Furthermore, data from one lobe could be scaled reasonably well with data from the other lobe only after switching the two short axes (and inverting the long axis *l*).

Table 2
Refinement statistics using twinned data.

Resolution range (Å)	30–3.0
Twin fraction	0.5
R factor†	22.1
R_{free}†	26.3
R.m.s.d. bond distances (Å)	0.007
R.m.s.d. bond angles (°)	1.2

† *R* factor and $R_{free} = \sum F_{obs} - F_{calc} / \sum F_{obs} \times 100$ for 95% of recorded data (*R* factor) or 5% of data (R_{free}).

This result suggested that the Dicer crystals were pseudo-merohedrally twinned and that the underlying symmetry was a special case of orthorhombic in which the length of the *a* axis is equal to that of the *b* axis. In this case, unit cells can be packed into the crystal lattice in two distinct orientations, which are related to each other by a 90° rotation about the *c* axis. The original crystals were likely to be composed of an equal distribution of the two unit-cell orientations such that the diffraction data contained equal contributions from each orientation. In the original crystals the twin domains are probably very small because in over 30 complete data sets collected we never encountered crystals that did not scale well as tetragonal, even when examining small wedges of data. This would produce extra symmetry along the *l* axis of the diffraction pattern and make the crystals appear to belong to the tetragonal crystal class.

These results confirmed our suspicion about the original crystals and also suggested a remedy for the twinning problem.

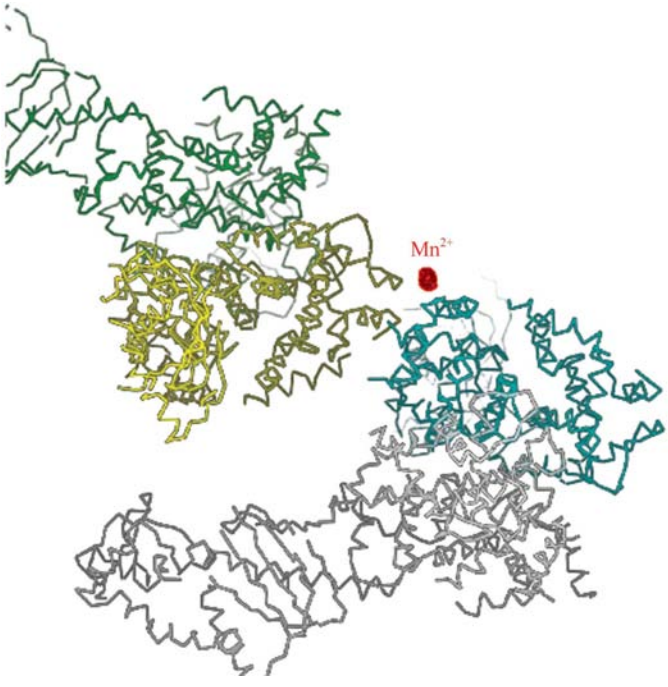

Figure 6
Intermolecular contacts between Dicer molecules in the $P2_12_12$ lattice. The four molecules in the asymmetric unit are colored green, yellow, blue and white, respectively. Red hatched density represents a 5σ peak observed by anomalous difference Fourier analysis of diffraction data measured at the Mn absorption edge.

By transferring Mn-grown crystals into less concentrated precipitant solutions, the macroscopically twinned crystals were partially dissolved. This treatment, similar to that used to dissect hemihedrally twinned crystals of bacteriorhodopsin (Efremov *et al.*, 2004), weakened the connection between each lobe, allowing the crystals to be readily dissected into their component single crystals for diffraction data collection (Fig. 4). The procedure was much more gentle than the physical separation of the crystals with a cat whisker described above. The resulting crystals yielded untwinned data sets belonging to space group $P2_12_12$. Data from single crystals revealed systematic absences along one of the short axes indicating a second screw axis, which had been masked in the twinned data sets because the two short axes (*h* and *l* when treated as $P2_12_12$) were superimposed. Heavy-atom sites were located by difference Fourier syntheses using diffraction data from $ErCl_3$-soaked crystals and phases calculated from a molecular-replacement solution using the backbone model built from the $P4_1$ map described above. 18 Er sites, eight of which had the same geometry as observed previously, were located within the unit cell at positions that readily accommodated four Dicer molecules in a $P2_12_12$ lattice. Electron-density map quality was good, leading to structure refinement at 3.3 Å resolution as described in Macrae *et al.* (2006).

3.3. Refinement against twinned native data

The Dicer crystals grown in the presence of $MnCl_2$ were always significantly smaller than those grown in the presence of $MgCl_2$. Furthermore, after dissection to separate the macroscopic twins, only tiny crystal shards remained. Owing to their small size, these crystals diffracted X-rays very weakly [$I/\sigma(I) < 11$ for all measured data], even when high-energy synchrotron radiation was used, and useful data could only be measured to a moderate resolution. For this reason, we wondered if it would be possible to produce a better model of Dicer by refinement against the stronger, higher resolution twinned data obtained from the larger $MgCl_2$-containing crystals.

The twinning operator used was (l, $-k$, h), which yielded a twinning fraction of 0.49 by least-squares refinement using *CNS*. The statistical method of Yeates (1997) produced a similar estimate of the twinning fraction. This near-perfect twinning of the original crystals unfortunately precluded refinement against the twinned data in *CNS* without introducing model bias (Yeates, 1997). The quality of the 3.0 Å electron-density map appeared to be better than the original map (Fig. 5) and the model refined with reasonable statistics after a single round of minimization using *CNS* (Table 2). However, OMIT maps clearly indicated that the introduced model bias made the high-resolution map less reliable (data not shown). Although refinement was successful it is clear to us that the model refined against the higher resolution twinned data is no better, and perhaps less reliable than, the original lower resolution untwinned model. Other refinement programs that enable refining against the twinned intensities

while applying the twin operation to the model could be used to avoid introducing model bias.

3.4. Packing analysis: influence of noncrystallographic symmetry on twinning

It is unclear why replacing $MgCl_2$ with $MnCl_2$ reduced twinning in the *Giardia* Dicer crystals. However, we noticed that while the short axes of the $MgCl_2$-grown crystals are of identical length (155.45 Å), even when the data were processed as orthorhombic (Table 1), the equivalent axes of the $MnCl_2$-grown crystals are slightly different (155.5 and 152.7 Å). This discrepancy makes the molecular spacings between the twin domains slightly different, which probably diminished the propensity of the crystal to twin and gave rise to the single-crystal lobes observed in the presence of $MnCl_2$. Indeed, seeding with non-twinned parts from dissected crystals in the presence of $MnCl_2$ produced single plate-like crystals. Unfortunately, these crystals were too thin and fragile to be useful for data collection. Inspection of anomalous difference maps calculated using diffraction data measured at the Mn edge revealed a Mn^{2+} ion situated between the two pairs of Dicer molecules in the crystallographic asymmetric unit (Fig. 6). One possibility is that the binding of this ion contributed to the slight change in lattice dimensions observed in the presence of $MnCl_2$.

We are also unable to fully explain why processing the original twinned data in space group $P4_1$ produced a semi-interpretable electron-density map. We did notice, however, that the asymmetric unit of the single orthorhombic crystals is composed of two pairs of Dicer molecules that are exactly related to each other by a 90° rotation and a quarter unit-cell translation about the long (*b*) axis. Thus, the asymmetric unit has symmetry that is similar and parallel to the twinning operator of the original crystals. As a result, the two twinning lattices share a common position for one of the Dicer molecule pairs, providing a simple way for the two twin domains to interact and interweave in the original twinned crystals. Indeed, examining the crystal lattice after rotating it 90° and translating by quarter of the unit cell, such that one pair of Dicer molecules falls directly onto the second pair, reveals reasonable packing interactions between the two lattices. By treating the twinned data as $P4_1$ we may have inadvertently generated an electron-density map that mimics the symmetry generated by the two superimposed twin domains. Crystal twinning is often correlated with the presence of noncrystallographic symmetry (NCS), particularly when the NCS operator is parallel with the twinning operator (Yeates, 1997).

The authors gratefully acknowledge Paul Adams, Jamie Cate, John Kuriyan, James Holton, Tom Alber and James Berger for helpful discussions during data processing and refinement. Kaihong Zhou provided outstanding technical support for the project.

References

Adams, P. D., Gopal, K., Grosse-Kunstleve, R. W., Hung, L.-W., Ioerger, T. R., McCoy, A. J., Moriarty, N. W., Pai, R. K., Read, R. J., Romo, T. D., Sacchettini, J. C., Sauter, N. K., Storoni, L. C. & Terwilliger, T. C. (2004). *J. Synchrotron Rad.* **11**, 53–55.
Barends, T. R. M. & Dijkstra, B. W. (2003). *Acta Cryst.* D**59**, 2237–2241.
Bernstein, E., Caudy, A. A., Hammond, S. M. & Hannon, G. J. (2001). *Nature (London)*, **409**, 363–366.
Blaszczyk, J., Tropea, J. E., Bubunenko, M., Routzahn, K. M., Waugh, D. S., Court, D. L. & Ji, X. (2001). *Structure*, **9**, 1225–1236.
Brünger, A. T., Adams, P. D., Clore, G. M., DeLano, W. L., Gros, P., Grosse-Kunstleve, R. W., Jiang, J.-S., Kuszewski, J., Nilges, M., Pannu, N. S., Read, R. J., Rice, L. M., Simonson, T. & Warren, G. L. (1998). *Acta Cryst.* D**54**, 905–921.
Dauter, Z. (2003). *Acta Cryst.* D**59**, 2004–2016.
Efremov, R., Moukhametzianov, R., Buldt, G. & Gordeliy, V. (2004). *Biophys. J.* **87**, 3608–3613.
Holton, J. & Alber, T. (2004). *Proc. Natl Acad. Sci. USA*, **101**, 1537–1542.
Ketting, R. F., Fischer, S. E., Bernstein, E., Sijen, T., Hannon, G. J. & Plasterk, R. H. (2001). *Genes Dev.* **15**, 2654–2659.
Macrae, I. J., Zhou, K., Li, F., Repic, A., Brooks, A. N., Cande, W. Z., Adams, P. D. & Doudna, J. A. (2006). *Science*, **311**, 195–198.
Otwinowski, Z. & Minor, W. (1997). *Methods Enzymol.* **276**, 307–326.
Padilla, J. E. & Yeates, T. O. (2003). *Acta Cryst.* D**59**, 1124–1130.
Potterton, E., McNicholas, S., Krissinel, E., Cowtan, K. & Noble, M. (2002). *Acta Cryst.* D**58**, 1955–1957.
Potterton, L., McNicholas, S., Krissinel, E., Gruber, J., Cowtan, K., Emsley, P., Murshudov, G. N., Cohen, S., Perrakis, A. & Noble, M. (2004). *Acta Cryst.* D**60**, 2288–2294.
Rudolph, M. G., Wingren, C., Crowley, M. P., Chien, Y. & Wilson, I. A. (2004). *Acta Cryst.* D**60**, 656–664.
Taylor, H. O. & Leslie, A. G. W. (1998). *CCP4 Newsl.* **35**, 9.
Vonrhein, C., Blanc, E., Roversi, P. & Bricogne, G. (2006). *Methods Mol. Biol.* **364**, 215–230.
Weiss, M. S. (2001). *J. Appl. Cryst.* **34**, 130–135.
Wilson, A. J. C. (1949). *Acta Cryst.* **2**, 318–321.
Wittmann, J. G. & Rudolph, M. G. (2007). *Acta Cryst.* D**63**, 744–749.
Yeates, T. O. (1988). *Acta Cryst.* A**44**, 142–144.
Yeates, T. O. (1997). *Methods Enzymol.* **276**, 344–358.
Yeates, T. O. & Fam, B. C. (1999). *Structure*, **7**, R25–R29.